Air Force Institute of Technology
AFIT Scholar

Faculty Publications

1-20-2021

Implications of Polarized Pupil Degradation Due to Focal Shifts in Dynamically Ranged Rayleigh Beacons

Steven M. Zuraski
Air Force Research Laboratory

Ethan VanTilburg

Matthew Wilson

Jack E. McCrae
Air Force Institute of Technology

Steven T. Fiorino
Air Force Institute of Technology

Follow this and additional works at: https://scholar.afit.edu/facpub

 Part of the Optics Commons

Recommended Citation

Steven M. Zuraski, Ethan VanTilburg, Matthew Wilson, Jack E. McCrae, and Steven T. Fiorino, "Implications of polarized pupil degradation due to focal shifts in dynamically ranged Rayleigh beacons," Appl. Opt. 60, 606-615 (2021). https://doi.org/10.1364/AO.405277

This Article is brought to you for free and open access by AFIT Scholar. It has been accepted for inclusion in Faculty Publications by an authorized administrator of AFIT Scholar. For more information, please contact richard.mansfield@afit.edu.

applied optics

Implications of polarized pupil degradation due to focal shifts in dynamically ranged Rayleigh beacons

Steven M. Zuraski,[1,2,*] Ethan VanTilburg,[3] Matthew Wilson,[3] Jack E. McCrae,[2] and Steven T. Fiorino[2]

[1]Air Force Research Laboratory, Sensors Directorate, 2241 Avionics Circle, Wright-Patterson AFB, Ohio 45433-7765, USA
[2]Air Force Institute of Technology, Department of Engineering Physics, Center for Directed Energy, 2950 Hobson Way, Wright-Patterson AFB, Ohio 45433-7765, USA
[3]Applied Optimization Inc. 3040 Presidential Drive, Fairborn, Ohio 45324, USA
*Corresponding author: steven.zuraski@us.af.mil

Received 14 August 2020; revised 9 December 2020; accepted 9 December 2020; posted 11 December 2020 (Doc. ID 405277); published 18 January 2021

A dynamically ranged pulsed Rayleigh beacon using sensed wavefronts across a system's pupil plane is proposed for tomographic quantification of the atmospheric turbulence strength. This method relies on relaying light from a telescope system's pupil plane to a wavefront sensor and having precise control of the light-blocking mechanisms to filter out scattered light from the unwanted scattering regions along the propagation path. To accomplish this, we tested and incorporated design features into the sensing system that we believe, to the best of our knowledge, are unique. Dynamically changing the range of the beacon source created focal shifts along the optical axis in the telescope sensing system. This effect induced polarization degradation in the optical pupil. As a result, polarization nonuniformity within the Pockels cell resulted in light leakages that corrupted the sensed data signals. To mitigate this unwanted effect, an analysis of the polarization pupil had to be completed for the range of possible Rayleigh beacon source distances, relating the change in polarization to the ability of a Pockels cell to function as an optical shutter. Based on the resultant polarization pupil analysis, careful design of the light relay architecture of the sensing system was necessary to properly capture sensed wavefront data from a series of intended ranges. Results are presented for the engineering design of the Turbulence and Aerosol Research Dynamic Interrogation System sensing system showing the choices made within the trade space and how those choices were made based on an analysis of the polarization pupil. Based on what we learned, recommendations are made to effectively implement a polarization-based Pockels cell shutter system as part of a dynamically ranged Rayleigh beacon system. © 2021 Optical Society of America under the terms of the OSA Open Access Publishing Agreement

https://doi.org/10.1364/AO.405277

1. INTRODUCTION

A. Motivation

Measuring atmospheric turbulence to correct for aberrations in an image has been of interest to the scientific community for a long time. Traditionally, a wavefront sensor is used to measure the corrections needed in the pupil plane of a system, but this provides no information about the turbulence strength profile along the path. It is a path-integrated measurement, but historically has been sufficient for adequate image correction. However, as ranges become farther, wide fields have become more desirable. In addition, as telescope apertures become larger, the turbulence effects become more pronounced and path-integrated techniques fail to provide adequate image correction [1]. Born out of a need, vertical profiling techniques were conceived, modeled, tested, and integrated in adaptive optics assisted imaging programs [2–4]. Two well accepted techniques to produce a vertical profile of atmospheric turbulence strength are scintillation detection and ranging (SCIDAR) and slope detection and ranging (SLODAR) [5,6]. These methods, among others, inform systems and researchers to some level of the path-resolved turbulence strength and aid in driving adaptive optics systems.

When scintillation and anisoplanatism become dominant effects, such as in deep turbulence, adaptive optics compensation becomes notably challenging. In deep turbulence, conventional adaptive optics schemes have inadequate performance. As such, new approaches must be conceived. Tyler [7] provides a summarizing quantification of some of the leading approaches. Of significance, multiconjugate adaptive

optics (MCAO) technology holds promise. In theory, MCAO systems could reduce and/or eliminate anisoplanatism. As a way to overcome the field-of-view limitations of conventional adaptive optics systems, Beckers in (1989) [8] proposed this MCAO concept. Shortly after that, in 1990 Tallon and Foy [9] introduced the concept of tomography to the problem set of atmospheric turbulence. The idea was to resolve the turbulence strength with altitude from independent measurements from a number of reference sources [10]. Using these MCAO concepts, three-dimensional turbulence representation can be obtained allowing for correction along any line of sight within the field of regard contained by the reference stars [11]. These techniques in conjunction with multiple laser guide stars systems have been accepted and employed at a number of observatories where large aperture and field-of-regard telescopes exist [12]. However, atmospheric tomography where there is a desire to compensate in real time for the rapidly changing distortions has led to computational burdens [13], whether for adapting to deep turbulence or a large telescope extended field-of-view requirements. With this in mind and using aspects from these concepts, a dynamically ranged Rayleigh beacon system concept was formulated with the goal to produce profiled strength estimates of turbulence along the optical path with a significantly lessened computational burden.

B. Problem Description

A method has been developed to sense the tomographic strength of optical turbulence along the viewing path of a telescope system [14]. This method employs a novel dynamically ranged Rayleigh beacon and is referred to as a research system called the Turbulence and Aerosol Dynamic Interrogation System (TARDIS) [15]. The dynamically ranged aspect of this system resulted in engineering challenges that had the potential to limit the utility of producing tomographic measurement estimations of the turbulence strength present along the viewing path. One challenge involved maintaining high-contrast ratio blocking by the optical shutter without light leakages for all dynamically ranged beacon configurations. Maintaining high-contrast ratio blocking posed a challenge unique to this sensing methodology because changing the range to the beacon inherently shifts the focus within the sensing system. The shift in focus is inherent to any dynamically ranged Rayleigh beacon concept. Alterative concepts to those employed by TARDIS exist. Most notable is that of a dynamic refocus system that does eliminate the light leakage problem [11,16,17]. However, using a dynamic refocus system does include moving parts within the sensing system, which could lead to a limiting factor in how fast a system like TARDIS could operate. This, in turn, would limit the tomographic range resolution for estimating turbulence strength. The TARDIS system does not focus the outgoing beacon at different ranges, but alternatively uses an on-axis collimated beacon where the range to the beacon is controlled purely by an electronic shutter in the sensing system. This solution has no physically moving parts. The TARDIS system uses a Pockels cell and control of the polarization state of the light to act as a fast optical shutter for the sensing system. However, the focal point in the sensing system can move due to the selected range to the beacon. These different ranges can affect the Pockels cell's ability to precisely control the polarization state across the system pupil, and the light blocking is consequently degraded. How the Pockels cell degrades in its ability to create an effective shutter is analyzed by understanding the polarization state across the telescope's relayed pupil. Subtle changes in the polarization state at points within the sensing system's pupil can result in light leakages that are strong enough to overcome the desired signal from the beacon. This effect is presented through mathematical theory, Zemax analysis specific to the TARDIS, and laboratory-based measurements using the Pockels cell shutter system from the TARDIS.

The blocking power of the Pockels cell engineering challenge arises from changing the range to the beacon source. Traditional beacon-based systems that do not intentionally change the range to the beacon, but still employ a Pockels-cell-based shutter do not have this problem because the optical component layout can be optimized for one specific range. Also, systems without a Pockels-cell-based shutter do not have this issue [18]. However, producing uniquely configured dynamically ranged beacon-based profiles without a Pockels-cell-based shutter would become more challenging due to the relatively fast timing requirements. Other solutions also have been explored. It has been proposed that Rayleigh beacons used as part of a constellation based scheme for MCAO can be effectively used in conjunction with a dynamic refocus sensing system. The refocusing system is used so that the return from each laser pulse can be sensed at a precalculated range-dependent sharp focal point. This technique will allow an increase in the brightness of the returned light to an optimal level and will potentially allow for higher altitude beacons than previously possible with traditional range-gating techniques [16,19]. This technique can provide enhancements to a dynamically ranged Rayleigh beacon system; however, it adds to the complexity of the system, requires mechanically moving parts, and is not absolutely required to perform dynamic-range gating. Alternatively, a novel sensing methodology has been proposed by Lloyd-Hart *et al.* [17] that suggests using the image-plane intensity distributions to extract pupil-plane phases. This methodology exploits the instantaneous point spread function (PSF) of the atmosphere and telescope optics in the downward path from the beacon. Phase recovered in this methodology from the extra focal images is a good measure of the pupil-plane distortions of the return path light from the beacon. This methodology was shown as feasible through simulation; however, it was mentioned that it would be reliant on a fast optical shutter such as that created by a Pockels cell. Consequently, since beacons from multiple ranges are required for this methodology to function, a similar issue will likely be discovered in practice. The main body of this paper will discuss the Pockels cell's ability to function as an optical shutter in the presence of a dynamically ranged Rayleigh beacon.

A dynamically ranged Rayleigh beacon system presents an engineering challenge: a shifting focus within the system. Particularly, this shifting focus can cause light leakages in a Pockels-cell-based optical shutter. This leakage arises from the ability of the Pockels cell to rotate the polarization field uniformly across the entire cross-section of the relayed light between two crossed polarizers within the system. The Pockels cell's ability to function as an optical shutter is addressed in the

remainder of the paper by analyzing the polarizing pupil in the system at key points along the optical path through simulation. These effects are further explored through experimentation, with the results demonstrating the Pockels cell blocking contrasts for multiple beacon ranges. From this, a recommendation is presented that will allow for mitigating changing focus effects on the Pockels cell's ability to function as a fast optical shutter. The analysis presented along with the recommendations provided provide a path forward to effectively use Pockels cells as fast optical shutters in the presence of a shifting focus within the sensing system. This allows for dynamically ranged Rayleigh beacon systems to produce higher resolution tomographic estimates of the turbulence strength along the viewing path produced from high-speed measurements not limited by physically moving parts.

2. TARDIS SYSTEM

The TARDIS is an optical sensing system based on dynamically changing the range between the collecting sensor and Rayleigh beacon during a static period of relatively unchanging turbulence-induced wavefront perturbations. A notional collecting scenario is shown in Fig. 1, where the idealized circular "beacons" are the air molecule and aerosol particle backscatter images captured at different distances from the collecting aperture based on laser pulsing and camera shutter speed. The TARDIS system uses an on-axis collimated outgoing pulsed laser beam where the range to the beacon is controlled through an electronically driven fast optical shutter. It is shown that there are overlapping and nonoverlapping atmospheric turbulence regions that affect the wavefront perturbations seen in each of the backscatter beacon images. These are used as part of an algorithm to deduce a discretized version of the refractive index structure parameter that is segmented based on the choice of beacon locations [20]. The TARDIS is comprised of a beam projection system, collecting telescope, and a sensor system. Within the sensor system, there is a beam relay and conditioning system that collimates and controls the size of the sensed light, a Pockels cell that acts as a fast shutter, and a Shack–Hartmann wavefront sensor that is comprised of a lenslet array and camera. These systems function in unison to control the light from the Rayleigh beacon so that the camera senses light from the desired ranges [14].

Key components of the sensing system are shown in the layout diagrams in Fig. 2. The flip mirror is aligned to the optical axis and folds light traveling through the telescope's central annulus. M1 through M5 are flat, turning mirrors used to fold the light within the confined space. An iris is used to block unwanted light. Ln is a negative lens that conditions the beam to an appropriate size. L1 and L2 are relay lenses that collimate and refocus the beam for relay through the polarizers, P1 and P2, and the Pockels cell, PC. L3 collimates the beam at a reduced size for input into the Shack–Hartmann wavefront sensor (SHWFS). Alternatively, for signal-to-noise ratio (SNR) investigations and increased sensitivity, the SHWFS can be replaced by a focusing lens and photodetector, labeled L4 and PD.

The Pockels cell used as a fast optical shutter is a crucial component that enables dynamic ranging of the Rayleigh beacon

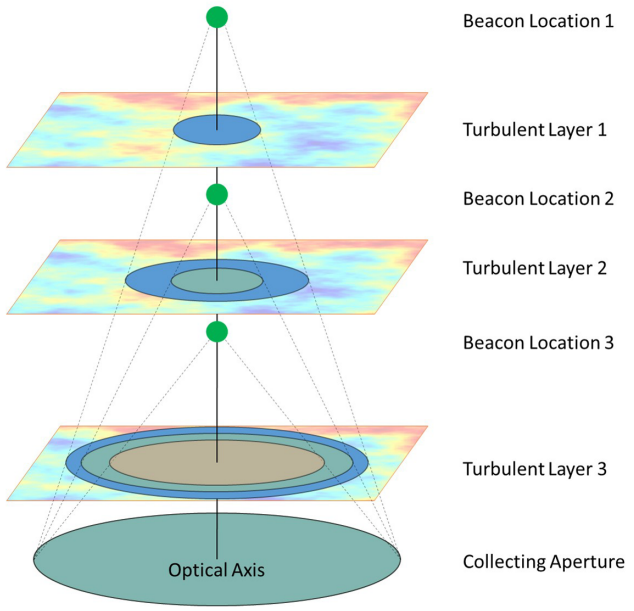

Fig. 1. Notional dynamic beacon collection scenario displaying a three-beacon collecting scenario where the beacon is placed a different ranges along the sensing system's optical axis.

source. The Pockels cell can be configured and controlled electronically using predefined configurations using inputs from a function generator in conjunction with control software provided by the manufacturer [21]. For the Pockels cell to function properly, the precise timing must be understood and the light-blocking contrast must be high to reject light from undesired ranges from the sensing system. The ability of the Pockels cell to function as a shutter is dominated by the uniformity of the electric field within the crystal, light leakages caused by unwanted birefringence within the crystal, quality of the polarizers used, the accuracy of the orientation of the polarizers used, and the divergence of the incident beam traveling through the Pockels cell [22]. For the TARDIS, the uniformity of the electric field was controlled well, resulting in a minimal effect. Birefringence within the Pockels cell crystal was unnoticeable. The quality and orientation accuracy of the polarizers were precisely measured and controlled. These qualities had minimal negative effects on the Pockels cell system's ability to function as an optical shutter. However, the divergence of the incident beam did play an important role and, consequently, the resultant light leakage effects had to be measured and mitigated. Ideally, the light should pass parallel to the crystal's optic axis for uniform field rotation to occur. Beams that have a finite divergence will not be uniformly retarded and light leakages will occur [22]. This effect can be understood further by analyzing the polarization pupil within the Pockels cell system for a range of possible divergence angles. A notional graphic of this effect is shown in Fig. 3. This analysis was done in Zemax [23]. Additionally, for the TARDIS, the ability to block light was measured from an experimental setup that simulated propagated light from a range of beacons distances. This was done using a lens system to emulate the telescope collection optics and a re-imaging lens to shift the focal point to emulate the dynamic-range beacon. The TARDIS sensing system was set up along the optical axis of this lens system

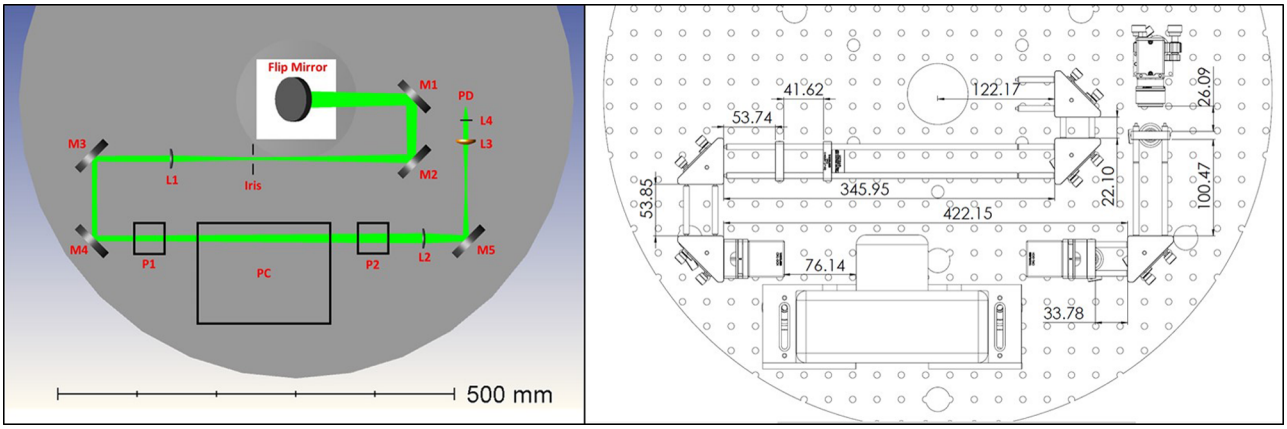

Fig. 2. Sensing system light path and physical layout.

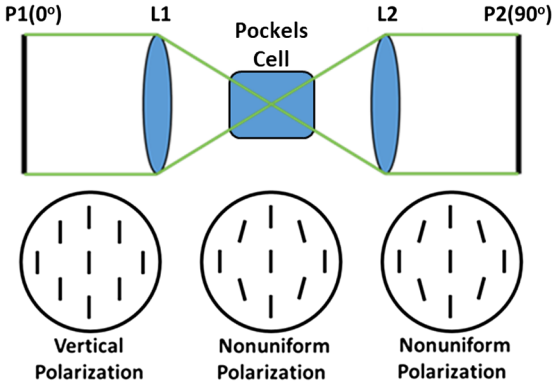

Fig. 3. Notional effect of converging or diverging beams on the polarization pupil.

Table 1. Input Parameters and Resultant Photon Counts for Example Beacon

Parameter	Value
Pulse Energy (mJ)	8
Wavelength (nm)	527
Atmospheric Pressure (mbar) 1 km, 2 km, 5 km, 10 km	898.75, 794.95, 540.2, 264.36
Atmospheric Temperature (K) 1 km, 2 km, 5 km, 10 km	281.65, 275.15, 255.65, 223.15
Area of receiving aperture (m^2)	1.17
Range (m)	1000, 2000, 5000, 10000
Receiver range gate length (m)	100, 200, 500, 1000
Expected photons at detector aperture	3.70×10^5, 1.67×10^5, 0.49×10^5, 0.14×10^5
Expected photons per subaperture	3302, 1495, 437, 123

such that the same effects could be measured in the laboratory as in the operational collection system. Results from both the mapping of the polarization pupil versus the divergence angle and the system's measured ability to block light from a range of beacon distances are presented in subsequent sections in this paper.

The SHWFS is used to measure the resultant phase of the incoming wavefront by zonal tilt, also known as slope measurements [16]. For the SHWFS to function for this use, the incoming light is required to have temporal brevity, such that a single focused spot is produced by the lenslet array of the SHWFS. This temporal brevity is controlled by the Pockels cell shutter system. If the shutter system is unable to block light from outside the desired time window effectively, light leakages will result in all pixels on the detector to become overtaken by unwanted light, effectively making SHWFS spot measurements impossible. This happens because the system is based on Rayleigh beacon technology, where the laser beacon energy is produced at the sensing system and is propagated along the system's optical axis of. Laser energy scattered from closer ranges to the sensing system will be stronger in intensity. One model that describes this is the Lidar equation. The Lidar equation can be expressed symbolically as

$$N(z) = \left(\frac{E\lambda}{hc}\right)(\sigma_B n(z)\Delta z)\left(\frac{A_R}{4\pi z^2}\right)(T_o T_A^2 \eta) + N_B, \quad \textbf{(1)}$$

where $N(z)$ is the expected number of photons detected, E is the laser pulse energy, λ is the optical wavelength, h is Planck's constant, c is the velocity of light, σ_B is the effective backscatter cross-section, $n(z)$ is the number density of the scattering particulates at range z, Δz is the receiver range gate length, A_R is the area of the receiving aperture, T_o is the transmission of the optical components, T_A is the one-way transmission of the atmosphere between the telescope and the beacon, η is the quantum efficiency of the detector, and N_B is the number of background and noise electrons. The Rayleigh backscatter cross-section and atmospheric density product is given by

$$\sigma_B n(z) = 3.6 \times 10^{-31}\frac{P(z)}{T(z)}\lambda^{-4.0117}, \quad \textbf{(2)}$$

where P is the atmospheric pressure at range z in millibars, and T is the atmospheric temperature at range in Kelvin [18]. Modeled values using the TARDIS system parameters are shown in Table 1. Transmission through the system was measured to be 27.24%, and the atmospheric transmission was modeled as 78%. The detector quantum efficiency was taken from the camera data sheet and modeled as 64%. A 12 × 12

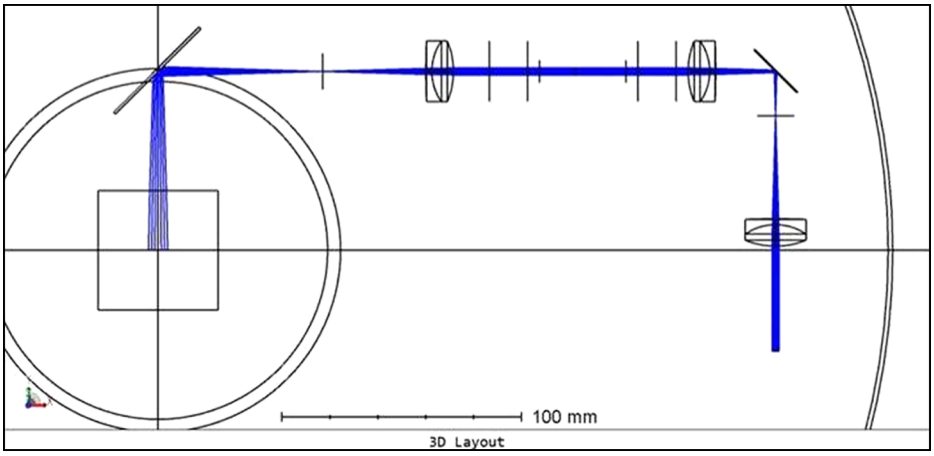

Fig. 4. Zemax ray analysis for the sensing system with light originating from an infinite range.

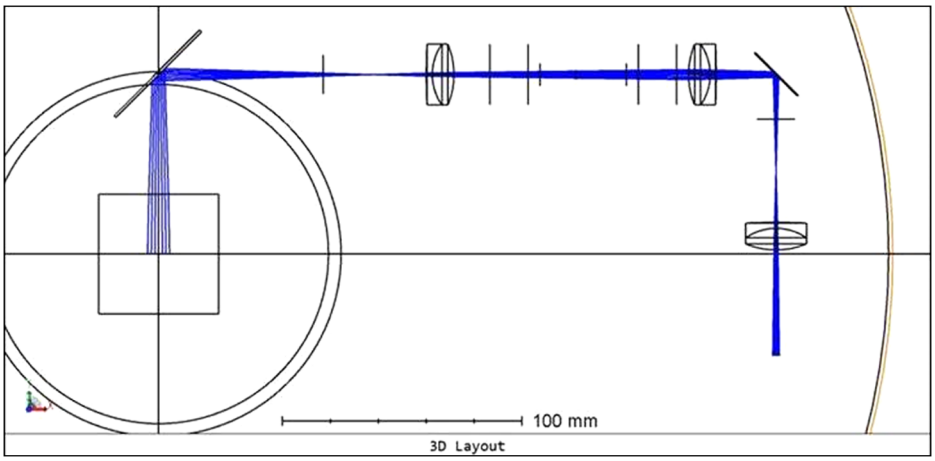

Fig. 5. Zemax ray analysis for the sensing system with light originating from a 5 km range.

subaperture array is used for this example. It is important to recognize that the TARDIS system is a proof-of-concept system and that the photon count could be increased by using a stronger laser source, which is commercially available but was not used due to the cost, choosing a shorter wavelength, increasing the collecting aperture size, or increasing the receiver range gate length.

3. FOCAL SHIFTS DUE TO DYNAMICALLY RANGED BEACON LOCATIONS

To take Rayleigh-beacon-based measurements and produce a tomographic estimation of the turbulence strength, the TARDIS is reliant on changing the range to the sensed beacon. This is done through an electronically configured shutter system that controls the timing of the light-blocking mechanisms while laser light propagates into the atmospheres along the optical axis of the sensing system [14]. Changing the range to the sensed beacon induces a focal shift in the sensing system that must be understood to take effective measurements. The optical beam relay was modeled in Zemax for the expected range of configurations [23]. Examples of some of the key configurations are shown in Figs. 4–6. A plot of the focal shift induced by the different ranges of beacon sources is presented in Fig. 7. The area to focus on in Figs. 4–6 is between the two polarizers where the Pockels cell resides, also depicted in Fig. 2. For a Pockels cell to function properly as an optical shutter, the light passing through the Pockels cell's aperture must be collimated or close to collimated [22]. For the TARDIS configuration set for beacon ranges from approximately 1.5 km to an infinite range, light rays passing through the Pockels cell are close to collimated. An infinite range and 5 km range is shown in Figs. 4 and 5. In both cases, the light is near collimated, with light rays only having minimal divergence. However, Fig. 6 highlights the 1 km range to the beacon that does significant focusing and diverging light rays within the Pockels cell. This divergence will consequently cause a nonuniform polarization state in the polarization pupil, as described in the Mathematical Interpretation section of this paper below and similarly highlighted by the polarization pupil image in Fig. 9. For the TARDIS, this will manifest as light leakages that do not effectively become shuttered for the close to the sensing system ranges, and will consequently have to be blocked by other means.

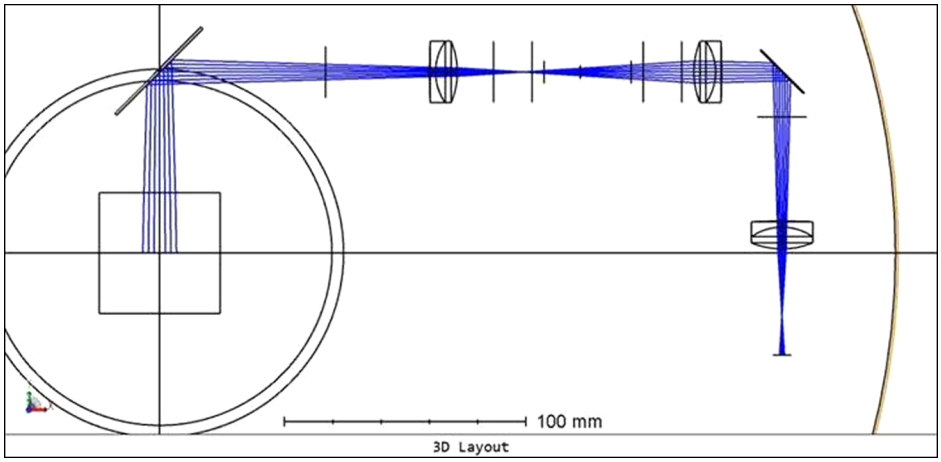

Fig. 6. Zemax ray analysis for the sensing system with light originating from a 1 km range.

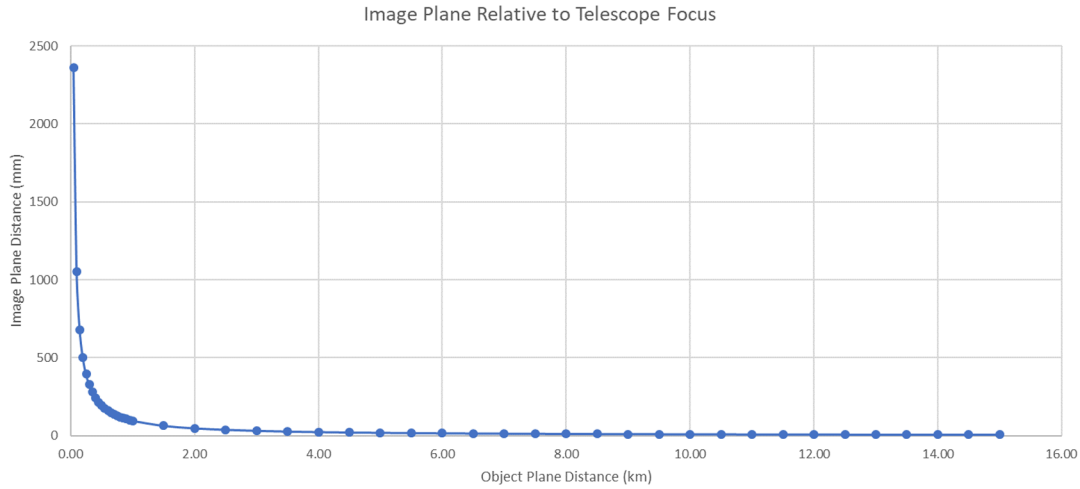

Fig. 7. Plot of the change in image plane location for beacons originating from varied distances showing significant movement at 1.5 km and below.

4. POLARIZATION PUPIL ANALYSIS

A. Mathematical Interpretation

The wavefront curvature through the Pockels cell must be minimized for the Pockels cell to perform well as an optical shutter, implying that beam passing through the crystal must have minimal angular divergence or beam focus. Light beams that have a finite divergence or focus will not be uniformly retarded by the Pockels cell. Consequently, the operation of the Pockels cell as an optical shutter will degrade due to light leakages. These light leakages can be strong enough to overcome the signal from the returned Rayleigh beacon [22].

The polarization pupil within the Pockels cell can be analyzed using Jones calculus following the methodologies presented by Ruoff and Totzeck [24] or Chipman [25]. A convenient way to describe a polarized field is by its Jones vector, **J**, which is comprised of the transverse electric field components E_1 and E_2, so

$$\mathbf{J} = \begin{pmatrix} E_x \\ E_y \end{pmatrix} = \begin{pmatrix} A_x e^{i\delta_x} \\ A_y e^{i\delta_y} \end{pmatrix} = A e^{i\delta_x} \begin{pmatrix} \cos\theta \\ \sin\theta e^{i\delta} \end{pmatrix}, \quad (3)$$

where A_i are amplitudes and δ_i are the phases, respectively. Pulling out the overall amplitude and arbitrary phase factor the Jones vector is written in the last form with $A_x = A\cos\theta$, $A_y = A\sin\theta$, and $\delta = \delta_y - \delta_x$. If $\delta = 0$, the light is linearly polarized with angle θ describing the orientation of the vibrational plane of the electric field. If $\delta \neq 0$, the polarization state is elliptical [24]. This is important because, for the Pockels cell to rotate the polarized field uniformly, the field must have uniform linear polarization across the whole pupil within the Pockels cell.

Converging or diverging light in a system can be viewed as coming from a lens. Analysis of the polarization pupil of this optical element can be thought of as a product of two well-understood optical elements: a linear retarder and a linear partial polarizer. These are used in their rotated forms as

$$\mathrm{J}_{\mathrm{pol}}(d, \psi_p) = \begin{pmatrix} 1 + d\cos 2\psi_p & d\sin 2\psi_p \\ d\sin 2\psi_p & 1 - d\cos 2\psi_p \end{pmatrix}, \quad (4)$$

$$\mathrm{J}_{\mathrm{ret}}(\phi, \psi_r) = \begin{pmatrix} \cos\phi - i\sin\phi\cos 2\psi_r & -i\sin\phi\sin 2\psi_r \\ -i\sin\phi\sin 2\psi_r & \cos\phi + i\sin\phi\cos 2\psi_r \end{pmatrix}, \quad (5)$$

where the orientation angles are ψ_p and ψ_r. The polarizer is characterized by the mean amplitude t and the relative amplitude difference $2d$. The retarder is characterized by the global phase factor Φ and the global phase retardation 2ϕ, with the fast axis corresponding to $(J_{\text{ret}})_{11}$. The Jones matrix for a lens is consequently represented as

$$\mathrm{J} = te^{i\Phi}\mathrm{J}_{\text{pol}}(d, \psi_p)\mathrm{J}_{\text{ret}}(\phi, \psi_r). \tag{6}$$

For the optical system, the Jones matrix is also a function of the pupil coordinates, commonly referred to as the Jones pupil or polarization pupil [24]. Using the described decomposition treatment for a lens, the Jones pupil within the Pockels cell can consequently be analyzed for the changing focal point effects that result from the operation of a dynamically ranged Rayleigh beacon.

The desired Jones pupil state within the Pockels cell is that of uniform linear polarization. At P1 in Fig. 2, the polarization is converted to a uniform linear polarization field. However, depending on the range to the Rayleigh beacon, the telescope's focal point in the sensing system will shift and consequently create converging or diverging light rays between the two polarizers, P1 and P2. Consequently, this affects the Pockels cell's function of uniformly rotating the full pupil of light and results in possible light leakages. These light leakages could be strong enough to raise the background noise levels to a point where the desired signal on the SHWFS is no longer detectable. To understand the effect of converging or diverging light rays, let us individually look at how a set of possible orientation angles affect the terms in [Eq. (6)] when applied to linearly polarized light. The partial polarizer and retarder are then governed by

$$\mathrm{J}_{\text{pol}}(d, \psi_p)\begin{pmatrix}1\\0\end{pmatrix} = \begin{pmatrix}1 + d\cos 2\psi_p\\ d\sin 2\psi_p\end{pmatrix}, \tag{7}$$

$$\mathrm{J}_{\text{ret}}(\phi, \psi_p)\begin{pmatrix}1\\0\end{pmatrix} = \begin{pmatrix}\cos\phi - i\sin\phi\cos 2\psi_r\\ -i\sin\phi\sin 2\psi_r\end{pmatrix}. \tag{8}$$

Analyzing the orientation angles between 0 and 90 deg, the polarization direction in the partial polarizer can result in a rotation. For the retarded, the polarization state can become elliptical. To summarize, when the incoming light is not parallel to the fast or slow axis for the partial polarizer or the bright or dark axis for the retarder, the polarization state of the light will become rotated or take on an elliptical form [24]. This outcome will further be shown through Zemax-based analysis focusing on these two observed effects in the polarization pupil.

B. Ray Tracing Polarization Pupil Analysis

The OpticStudio software produced by Zemax [23] was used to demonstrate how the polarization state can change across a pupil when light rays become converging or diverging. This analysis was designed to investigate a set of possibilities that would be analogous to convergent or divergent rays experienced by the TARDIS system due to the focal point shifting in the sensing system as a result of changing the range of the beacon. The analysis was set up for a wavelength of 527 nm with a uniform vertical polarization set to the entire entrance pupil. The polarization pupil function within the OpticStudio software was used

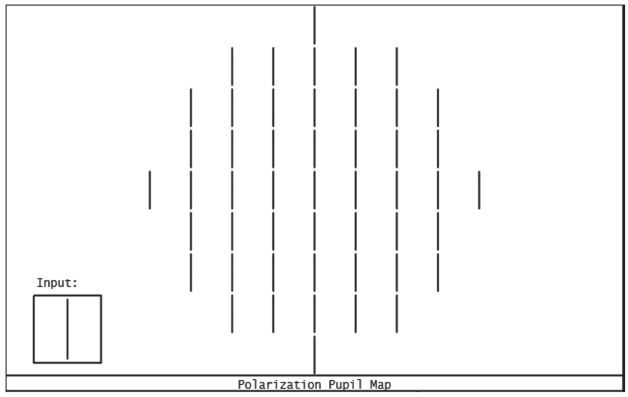

Fig. 8. Zemax polarization pupil map for a collimated beam subjected to vertical polarization input.

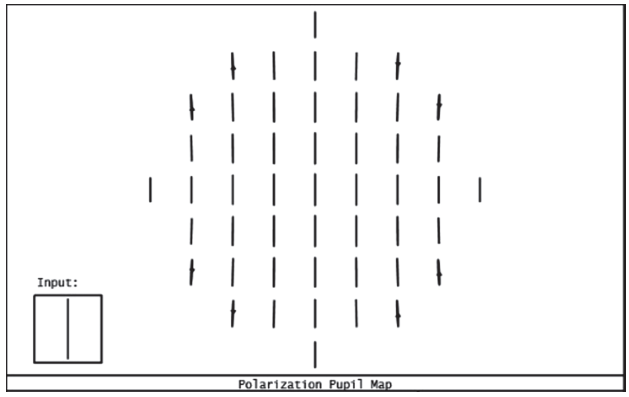

Fig. 9. Zemax polarization pupil map for a convergent beam subjected to vertical polarization input.

to evaluate how the polarization changes at the exit pupil of the system. An ensemble of simulations was set up to investigate convergent and divergent rays for a series of f-number lens setups. Changing the f-number had the effect of showing the enhanced effect on peripheral rays, showing the susceptibility to deviation from linear polarization. Figure 8 shows the default state for a system that is perfectly collimated, where all rays have vertical polarization. Figure 9 shows an example case of how rays toward the edge of the system's pupil stray from linear polarization and become tilted and elliptical.

Within the OpticStudio software, multiple data fields can be used to quantify the polarization change from the input to the exit pupil of the system. The polarization data fields of E_x and E_y were used for this analysis. For vertical polarization, E_x will equal 0 and E_y will equal 1. Any deviation from these values will indicate that part of the pupil no longer has pure vertical polarization and has become tilted with a small degree of elliptical polarization. Because convergent and divergent rays across the system's pupil do not uniformly change in polarization, the average and standard deviation metrics of the vertical polarization values were used. Figures 10 and 11 shows the change of these value versus the f-number of the system. The mean difference and standard deviation from the linear polarization state were calculated from the ensemble of discrete points for each f-number system. Examples of the discrete points sampled are shown in Figs. 8 and 9. This data presents a trend: the higher

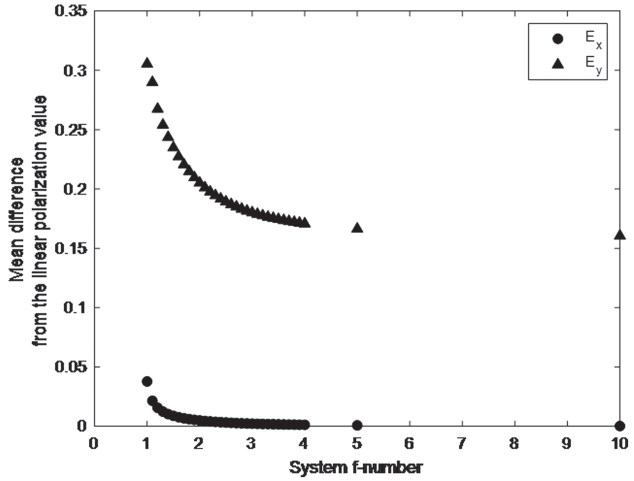

Fig. 10. Mean difference of E_x and E_y from the linear polarization value for system f-numbers from 1 to 10.

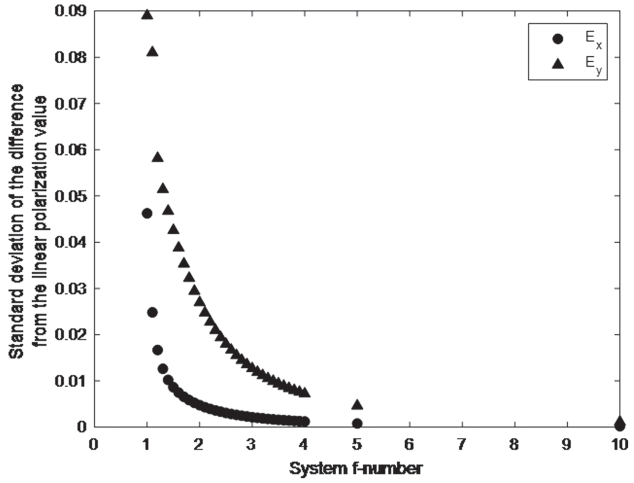

Fig. 11. Standard deviation of E_x and E_y from the difference from the linear polarization value for system f-numbers from 1 to 10.

effective f-number systems deviate less from the input state of uniform vertical polarization across the system's pupil.

C. Sensing System Laboratory Measurements

Laboratory measurements were taken looking at the light throughput to analyze the ability of the Pockels cell to function as an optical shutter in the presence of focal point shifts in the sensing system. A light relay system was set up to mimic the input to the sensing system in Fig. 2. Input laser lights were injected into this system with a reimaging system such that the focal shifts of incoming light due to changing the range to the beacon could be emulated. Emulated ranges being tested were 1000 m, 1200 m, 1500 m, and near-infinite. A near-infinite range was used because it is in the part of the curve in Fig. 7, where a minimal change in the system's focal point is exhibited.

Data was collected using this setup with the Pockels cell in the shuttered mode for these emulated ranges by recording the power measured by a photodiode and calculating the voltage by

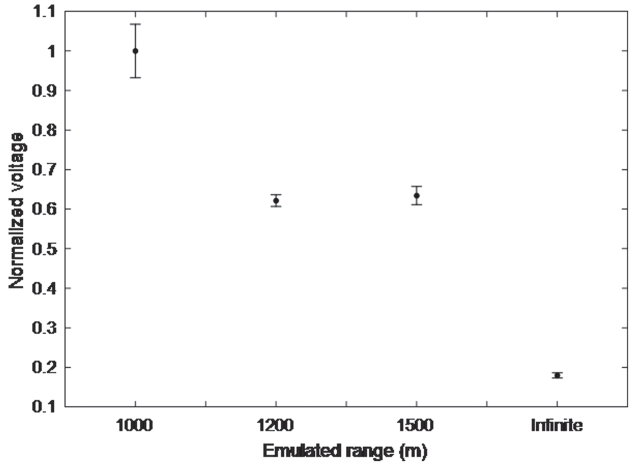

Fig. 12. Plot showing the results from laboratory measurements of the throughput of the sensing system for emulated ranges of 1000 m, 1200 m, 1500 m, and near-infinite.

$$V = \frac{P \times R}{R_s}, \tag{9}$$

where P is the power measured in watts, R is the selected resistance in ohms on the device, and R_s is the responsivity of the photodiode in watts per ampere. Multiple measurements were taken for each range setting, and each measurement was averaged for a period on the device long enough to reach a stable state. The results are shown in Fig. 12. The Pockels cell was chosen to be in the shuttered mode to achieve a measurement representative of the blocking ability. The idea was that when the light is near collimated like that for an infinite range setup, the light-blocking ability should be high and would yield a small value on the photodiode. Conversely, the blocking ability would be lessened when light rays are converging within the Pockels cell. This hypothesized trend is shown in Fig. 12. The error bars are two standard deviations from the mean of the measured data. A nonzero value is present for a near-infinite source setup. This is likely due to the high-intensity light source used in the laboratory and small imperfections and orientation errors in the Pockels cell and the polarizers.

5. DISCUSSION

Our laboratory setup allowed measurement of the optical throughput of a 527 nm laser through the sensing system with a reimaging system input to simulate the beam focusing conditions of the dynamically ranged Rayleigh beacon of the TARDIS. This experiment measured the light-blocking ability of the sensing system based on changing the convergence or divergence of the light rays as they traveled through the Pockels cell. Alterations for a laboratory-based setup were made compared to an on-sky TARDIS device. These included increasing the laser power injected to enable easily quantifiable and distinguishable measurements, and the use of a photodiode in place of the Shack–Hartmann wavefront sensor. These two laboratory accommodations are not believed to influence the resulting trends. It was observed that shorter emulated ranges exhibited larger measurement values, indicating that less light was able to be blocked by the Pockels cell shutter system.

Since the Pockels cell shutter system relies on manipulating the state of polarization between two linear polarizers, it was theorized that the state of the polarization pupil between the two linear polarizers within the Pockels cell aperture was not uniform. The Zemax modeling of the system supports this theory. As the focal point shifts toward the Pockels cell, the light rays become less collimated as they pass through the Pockels cell. The light rays that are furthest from the optical axis are most affected and exhibited a change of state from vertical linear polarization to tilted elliptical polarization. This elliptization was quantified through the Zemax models by extracting the change in the E_x and E_y terms for each data point within the polarization pupil. From this, a trend could be gleaned. As the focusing power increased, the change in the polarization terms away from the optical axis had a greater magnitude change. This focusing power is analogous to near to the sensing system beacon ranges for the TARDIS. Consequently for these scenarios, the light will not be effectively blocked by the Pockels-cell-based shutter system.

Without alternative mitigation techniques, the beacon ranges will be limited for a dynamically refocused Rayleigh-guide-star-based turbulence profiling system. The farthest beacons will be limited by the SNR limitations of the system, and the near beacons will be limited by light leakages produced from the polarization-based optical shutter not being able to maintain a uniform polarization state across the pupil. Unwanted light from outside the beacon range can be blocked by the use of special filters and lower speed physical or electronic shutters. Then the Pockels cell shutter only has to block light from a subrange closer to the intended beacon range. Specific to the TARDIS, ranges that are below approximately 1500 m start to exhibit light leakages, so dynamic ranging will be difficult, and the signal will have to overcome a more substantial source noise.

There are alternative mitigation techniques and system design choices that can help lessen the negative effect of light leakages stemming from nonuniformity in the polarization pupil. Suggested by Georges *et al.*, a dynamic refocus system can alter the angle of the light rays and maintain collimation between crossed polarizers within a Pockels-cell-based fast optical shutter. This system eliminates the light leakage issues and also effectively extends the useful range of possibilities to use Rayleigh beacons [19]. However, this comes at the cost of added complexity and moving parts within the sensing system. There are also simpler measures that can be taken to lessen the effective light leakages due to nonuniformity in the polarization pupil. One such method would be to use longer focal length relay lenses that are oversized and designed to handle Rayleigh beacons from both near and far ranges. This does not eliminate the problem, but it can lessen its effect. If employing this mitigation concept, the close ranges will likely result in a beam that is relayed through the system with a large effective beam radius. Many clear apertures of Pockels cells are quite small by design so that the high-voltage-induced polarization rotation can be enacted across the whole beam. The sensing system's beam reduction optics must be balanced to accommodate for close Rayleigh beacon ranges and the size of the mapped lenslets, which must be smaller than the effective Fried parameter r_o of the environment being sensed. These criteria can be used to produce an accurate r_o estimate [20].

6. CONCLUSION

Induced focal shifts in the TARDIS sensing system between subsequent neighboring beacons due to the process of changing the range to the Rayleigh beacon causes potential degradation from linear polarization of the polarized pupil present within the Pockels-cell-based optical shutter. This degradation from linear polarization manifests itself as a slightly rotated elliptical polarization state and is characterized by Jones calculus applied at each discrete point within the pupil. The amount of change was calculated using Zemax-based software specific to varied converging ray angles representative of what the TARDIS system could experience, especially at very low altitude beacon range choices. The trends found through the Zemax-based analysis were verified through an experimental setup that simulated beacon ranges where the polarization state change would be detrimental to the Pockels-cell-based optical shutter to adequately block light. The light leakages through the optical shutter under low altitude beacon ranges proved to be large enough to overwhelm a Shack–Hartmann wavefront sensor measurement by increasing the background signal. Based on the knowledge gained through our analysis, strategies have been developed to minimize the unwanted effects leading to light leakages. We believe the easiest strategy to mitigate the light leakage is a configuration choice that keeps the lowest beacon above 1500 m during the data collection operations. However, interesting turbulence strength changes can happen slightly below 1500 m, specifically around the boundary layer where a turbulence strength inversion typically occurs. As a recommendation, a minor design change of extending the focal length of the lenses in the relay system and effectively stretching the light relay to lessen the converging ray angles within the Pockels-cell-based optical shutter could be implemented that would also mitigate the cause of the light leakages and lower the effective beacon range where data could be collected. This would have a small negative effect specific to the TARDIS as space on the optical breadboard is limited and this strategy would physically take up more space. Finally, methods suggested by researchers at the University of Arizona that use a dynamic refocusing system would correct for all identified causes of light leakages due to focal shifts in the system. This strategy, however, does add significant complexity to the system and also would take up too much space on the TARDIS breadboard. However, for future TARDIS-like sensors that are not limited by breadboard space, an ideal solution would be a dynamic refocusing element that could operate at the same speed as the range changes employed by dynamically ranging the Rayleigh beacon.

Funding. Air Force Research Laboratory (FA8650-11-D-1186).

Acknowledgment. This work was supported by the Air Force Research Labs Sensors Directorate.

Disclosures. The authors declare no conflicts of interest.

REFERENCES

1. S. Bose-Pillai, B. Wilson, J. Krone, A. Archibald, B. Elmore, J. McCrae, and S. Fiorino, "Profiling atmospheric turbulence using dual-camera imagery of non-cooperative targets," Proc. SPIE**11506**, 115060J (2020).

2. J. Valenzuela, C. Béchet, A. Garcia-Rissmann, F. Gonté, J. Kolb, M. Louarn, B. Neichel, P. Madec, and A. Guesalaga, "Turbulence profiling methods applied to ESO's adaptive optics facility," Proc. SPIE **9148**, 91481X (2014).
3. A. Guesalaga, J. Kolb, R. Donaldson, J. Valenzuela, S. Oberti, B. Neichel, J. Paufique, and P. Madec, "An on-line turbulence profiler for the AOF: on-sky results," Proc. SPIE **10703**, 107032D (2018).
4. A. Reeves, R. Myers, T. Morris, A. Basden, N. Bharmal, S. Rolt, D. Bramall, N. Dipper, and E. Younger, "DRAGON, the Durham real-time, tomographic adaptive optics test bench: progress and results," Proc. SPIE**9148**, 91485U (2014).
5. R. Avila, J. Vernin, and E. Masciadri, "Whole atmospheric-turbulence profiling with generalized scidar," Appl. Opt. **36**, 7898–7905 (1997).
6. T. Butterley, R. Wilson, and M. Sarazin, "Determination of the profile of atmospheric optical turbulence strength from SLODAR data," Mon. Not. R. Astron. Soc.**369**, 835–845 (2006).
7. G. Tyler, "Adaptive optics compensation for propagation through deep turbulence: a study of some interesting approaches," Opt. Eng.**52**, 021011 (2012).
8. J. Beckers, "Detailed compensation of atmospheric seeing using multiconjugate adaptive optics," Proc. SPIE**1114**, 215–219 (1989).
9. M. Tallon and R. Foy, "Adaptive telescope with laser probe: isoplanatism and cone effect," Astron. Astrophys. **235**, 549–557 (1990).
10. R. Ragazzoni, E. Diolaiti, J. Farinato, E. Fedrigo, E. Marchetti, M. Tordi, and D. Kirkman, "Multiple field of view layer-oriented adaptive optics-nearly whole sky coverage on 8 m class telescopes and beyond," Astron. Astrophys. **396**, 731–744 (2002).
11. C. Baranec, M. Lloyd-Hart, N. Milton, T. Stalcup, Jr., J. Georges, III, M. Snyder, N. Putnam, and J. Angel, "Progress towards tomographic wavefront reconstruction using dynamically refocused Rayleigh laser beacons," Proc. SPIE**5490**, 1129–1137 (2004).
12. M. Hart, N. Milton, K. Powell, C. Baranec, T. Stalcup, D. McCarthy, and C. Kulesa, "Wide-field image compensation with multiple laser guide stars," Proc. SPIE **7468**, E32 (2009).
13. R. Ramlau, D. Saxenhuber, and M. Yudytskiy, "Iterative reconstruction methods in atmospheric tomography: FEWHA, Kaczmarz and gradient-based algorithm," Proc. SPIE**9148**, 91480Q (2014).
14. S. Zuraski, S. Fiorino, E. Beecher, N. Figlewski, J. Schmidt, and J. McCrae, "Electro-optic testbed utilizing a dynamic range gated Rayleigh beacon for atmospheric turbulence profiling," Proc. SPIE**10002**, 1000207 (2016).
15. S. Zuraski, E. Beecher, C. Carr, T. Payne, A. Battle, L. Guliano, and S. Fiorino, "Turbulence and aerosol research dynamic interrogation system testing," in *Adv. Maui Opt. and Space Surveillance Technol. Conf.* (2018).
16. J. R. P. Angel, "Dynamic refocus for laser beacons," in *Science with the LBT, in Sponsored by the Max Planck Society and the LBT Beteiligungsgesellschaft, Proceedings of a Workshop held at Ringberg Castle*, Bavaria, July, 2000, pp. 21–25.
17. M. Lloyd-Hart, S. Jefferies, E. Hege, and J. R. P. Angle, "New approach to Rayleigh guide beacons," Proc. SPIE**4007**, 277–283 (2000).
18. J. W. Hardy, *Adaptive Optics for Astronomical Telescopes* (Oxford University, 1998).
19. J. A. Georges, P. Mallik, T. Stalcup, J. R. P. Angle, and R. Sarlot, "Design and testing of a dynamic refocus system for Rayleigh laser beacons," Proc. SPIE **4839**, 473–483 (2003).
20. S. Zuraski, E. Beecher, J. McCrae, and S. Fiorino, "Turbulence profiling using pupil plane wavefront data derived fried parameter values for a dynamically ranged Rayleigh beacon," Opt. Eng. **59**, 081807 (2020).
21. Eksma Optics, "Ultrafast pulse picking systems," eksmaoptics.com/out/media/EKSMA_Optics_Pulse_Picking_Systems.pdf.
22. R. Goldstein, "Pockels cell primer," Laser Focus**34**, 21 (1968).
23. Zemax Optical Studio, "Optical design and simulation software," http://www.zemax.com.
24. J. Ruoff and M. Totzeck, "Orientation Zernike polynomials: a useful way to describe the polarization effects of optical imaging systems," J. Micro/Nanolithography, MEMS, MOEMS **8**, 031404 (2009).
25. R. A. Chipman, "Polarization analysis of optical systems, II," Proc. SPIE**1166**, 79–94 (1990).